Available online at www.sciencedirect.com
SCIENCE DIRECT®
International Journal of Thermal Sciences 43 (2004) 1101–1106
International Journal of Thermal Sciences
www.elsevier.com/locate/ijts

Performance analysis and optimum criteria of an irreversible Braysson heat engine

Yinghui Zhou [a], S.K. Tyagi [a,b], Jincan Chen [a,*]

[a] *Department of Physics, Xiamen University, Xiamen 361005, People's Republic of China*
[b] *Centre for Energy Studies, Indian Institute of Technology, Delhi New Delhi 110016, India*

Received 10 November 2003; received in revised form 23 February 2004; accepted 23 February 2004
Available online 21 April 2004

Abstract

An irreversible cycle model of a Braysson heat engine operating between two heat reservoirs is used to investigate the performance of the cycle affected by the finite-rate heat transfer between the working fluid and the heat reservoirs, heat leak loss between the heat reservoirs and irreversibility inside the cycle. The specific power output is maximized with respect to the cycle temperatures along with the isobaric temperature ratio. The specific power output is found to be a decreasing function of the internal irreversibility parameter and isobaric temperature ratio while there exist the optimal values of the state point temperatures at which the specific power output attains its maximum value for a typical set of operating parameters. Moreover, the maximum specific power output and other cycle parameters are calculated for different sets of operating conditions. The optimally operating regions of the important parameters in the cycle are determined. The results obtained here may provide some useful criteria for the optimal design and performance improvement of a realistic Braysson heat engine.

Keywords: Braysson heat engine; Multi-irreversibilities; Specific power output; Thermal efficiency; Optimally operating region; Optimum criterion

1. Introduction

The Braysson cycle is a hybrid power cycle based on a conventional Brayton cycle for the high temperature heat addition while adopting the Ericsson cycle for the low temperature heat rejection as proposed and investigated by Frost et al. [1] using the first law of thermodynamics. Very recently, some workers have investigated the performance of an endoreversible Braysson cycle [2–4] and a mirror cycle [5] based on the analysis of Brayton [6–23] and Ericsson [24–28] cycles by using the concept of finite time thermodynamics [29–38] for a typical set of operating conditions and obtained some significant results.

In real thermodynamic cycles, there often exist other irreversibilities besides finite-rate heat transfer between the working fluid and the heat reservoirs. For example, the heat leak loss between the heat reservoirs and internal dissipation of the working fluid are also two main sources of irreversibility. In the present paper, we will study the influence of multi-irreversibilities on the performance of a Braysson heat engine cycle.

2. An irreversible Braysson cycle

An irreversible Braysson cycle working between a source and a sink of infinite heat capacities is shown on the T–S diagram of Fig. 1. The external irreversibilities are due to the finite temperature difference between the heat engine and the external reservoirs and the direct heat leak loss from the source to the sink while the internal irreversibilities are due to nonisentropic processes in the expander and compressor devices as well as due to other entropy generations within the cycle. The working fluid enters the compressor at state point 4 and is compressed up to state point $1S/1$ in an ideal/real compressor, and then it comes into contact with the heat source and is heated up to state point 2 at constant pressure. After that the working fluid enters the turbine at state point 2 and expands up to state point $3S/3$ in an ideal/real expander/turbine, it rejects the heat to the heat sink at constant temperature and enters the compressor at state point 4, thereby, completing the cycle. Thus we study

* Corresponding author.
E-mail address: jcchen@xmu.edu.cn (J. Chen).

1290-0729/$ – see front matter
doi:10.1016/j.ijthermalsci.2004.02.008

Nomenclature

A	area	m^2	
c_P	specific heat	$kJ{\cdot}kg^{-1}{\cdot}K^{-1}$	
k_0	heat leak coefficient	$kW{\cdot}K^{-1}$	
$\dot{m}$	mass flow rate of the working fluid	$kg{\cdot}s^{-1}$	
P	specific power output	$kW{\cdot}m^{-2}$	
P^*	dimensionless specific power output		
Q	heat transfer rate	kW	
Q_0	heat leak loss	kW	
R	internal irreversibility parameter		
S	entropy	$kJ{\cdot}K^{-1}$	
T	temperature	K	
U	overall heat transfer coefficient	$kW{\cdot}m^{-2}{\cdot}K^{-1}$	
x	isobaric temperature ratio		
1, 2, 3, 4	state points		

Greeks symbol

η	efficiency

Subscripts

H	heat source/hot-side
L	sink/cold-side
max	maximum
m	optimum
η	at maximum thermal efficiency

the 4–1–2–3–4 closed cycle of an irreversible Braysson heat engine coupled with the heat reservoirs of infinite heat capacities at temperature T_H and T_L, respectively.

Assuming the working fluid as an ideal/prefect gas and the heat exchangers as counter flow configurations, the heat transfer to and from the heat engine following Newton's Law of heat transfer will be

$$Q_H = \frac{U_H A_H (T_2 - T_1)}{\ln((T_H - T_1)/(T_H - T_2))} = \dot{m} c_P (T_2 - T_1) \tag{1}$$

and

$$Q_L = U_L A_L (T_3 - T_L) \tag{2}$$

where U_J and A_J $(J = H, L)$ are the overall heat transfer coefficients and areas on their respective heat exchangers, T_i $(i = 1, 2, 3)$ are the temperatures of the working fluid at state points 1, 2 and 3, and $\dot{m}$ and c_P are, respectively, the mass flow rate and specific heat of the working fluid.

According to Fig. 1, it is reasonable to consider some heat leak loss directly from the source to the sink, which may be expressed as [26,27,30]

$$Q_0 = k_0 (T_H - T_L) \tag{3}$$

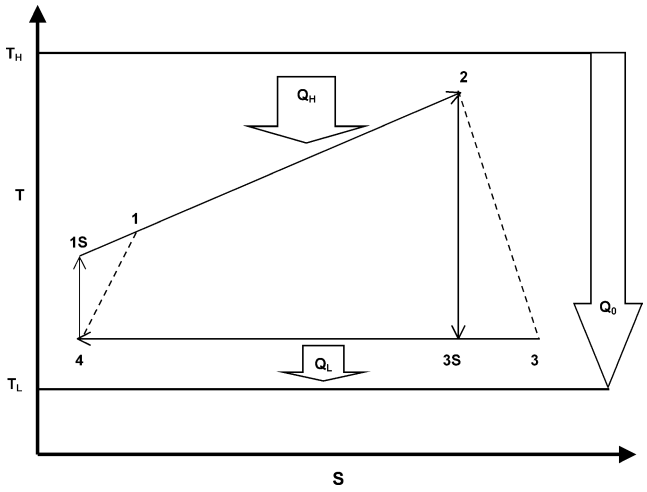

Fig. 1. The T–S diagram of an irreversible Braysson heat engine cycle.

where k_0 is the heat leak coefficient. In addition, it is very significant to further consider the influence of irreversible adiabatic processes and other entropy generations within the cycle. Using the second law of thermodynamics for this cycle model, we have

$$\dot{m} c_P \ln(x) - U_L A_L (T_3 - T_L)/T_3 < 0$$
$$\Longrightarrow \dot{m} c_P R T_3 \ln(x) = U_L A_L (T_3 - T_L) \tag{4}$$

where $x = T_2/T_1$ is the isobaric temperature ratio and R is the internal irreversibility parameter which is greater than unity for a real cycle and defined as

$$R = \frac{S_3 - S_4}{S_2 - S_1} = \frac{U_L A_L (T_3 - T_L)/T_3}{\dot{m} c_p \ln(x)} > 1 \tag{5}$$

where S_1, S_2, S_3 and S_4 are the entropy of the working fluid at state point 1, 2, 3 and 4, respectively. When the adiabatic processes are reversible and other entropy generations within the cycle are negligible, $R = 1$ and the cycle becomes an endoreversible cycle, in which the irreversibility is only due to finite temperature differences between the heat engine and the external reservoirs and the heat leak loss between the heat reservoirs. When $R = 1$ and the heat leak loss is negligible, the cycle model is directly simplified as that adopted in Refs. [2,3].

3. The expressions of several parameters

Using Eqs. (1)–(3) and (5), we can derive the expressions of the specific power output and thermal efficiency, which are, respectively, given by

$$P = \frac{Q_H - Q_L}{A} = \frac{U_H [(x-1)T_1 - R T_3 \ln x]}{a T_3/(T_3 - T_L) + b} \tag{6}$$

and

$$\eta = \frac{Q_H - Q_L}{Q_H + Q_0} = \frac{[(x-1)T_1 - R T_3 \ln x]}{(x-1)T_1 + \frac{k_0 (T_H - T_L)}{U_H A} [a T_3/(T_3 - T_L) + b]} \tag{7}$$

where $a = (U_H/U_L)R\ln x$, $b = \ln[(T_H - T_1)/(T_H - T_1 x)]$ and $A = A_H + A_L$ is the total heat transfer area of the cycle. Using Eqs. (1)–(3) and (5), we can also derive the expressions of the ratios of the hot- and cold-side heat exchanger areas to the total heat exchanger area as

$$\frac{A_H}{A} = \frac{b}{aT_3/(T_3 - T_L) + b} \tag{8}$$

and

$$\frac{A_L}{A} = \frac{aT_3/(T_3 - T_L)}{aT_3/(T_3 - T_L) + b} \tag{9}$$

Using the above equations, one can analyze the optimal performance of a realistic Braysson heat engine.

4. Optimal performance characteristics

It is seen from Eq. (6) that the specific power output is a function of two variables (T_1, T_3) for given values of the isobaric temperature ratio x and other parameters. Using the extremal condition $\partial P/\partial T_3 = 0$ and Eq. (6), it can be proven that when the specific power output is in the optimal states, the temperature T_3 should satisfy the following equation

$$T_3 = T_L \frac{b + \sqrt{b(c-a) + ac}}{a + b} \tag{10}$$

where $c = (U_H/U_L)(x-1)T_1/T_L$. Using Eqs. (6) and (10), one can generate a three-dimensional graph, as shown in Fig. 2, where $P^* = P/(U_L T_L)$ is the dimensionless specific power output and the parameters $T_H = 1200$ K, $T_L = 300$ K, $R = 1.1$ and $U_H/U_L = 1$ are chosen. It is seen from Fig. 2 that the specific power output first increases and then decreases as T_1 increases. It shows clearly that there is an optimal value of T_1 at which the specific power output attains its maximum value for a given set of operating parameters, as shown in Fig. 3, where the values of T_{1m} and $P^*_{\max}$ are listed in Table 1, which also gives the optimal values of other parameters at the maximum specific power output. It is also seen from Figs. 2 and 3 that the specific power output is a monotonically decreasing function of x and R. This point is easily expounded from the theory of thermodynamics. Because the larger the isobaric temperature ratio x and internal irreversibility parameter R are, the larger the total irreversibility in the cycle and consequently the smaller the specific power output.

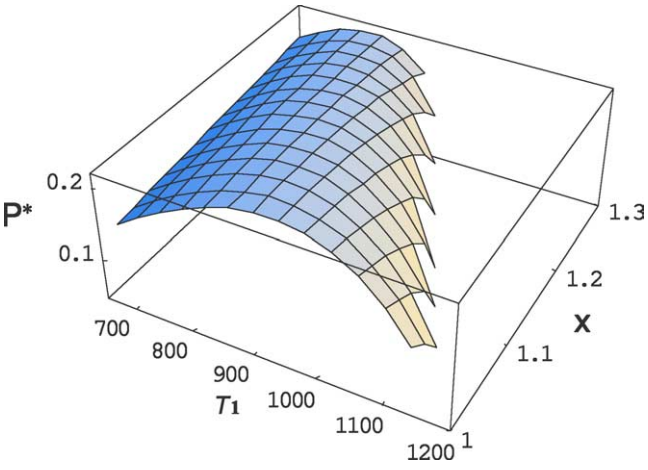

Fig. 2. The variation of the dimensionless specific power output P^* with respect to temperature T_1 and isobaric temperature ratio x, where the parameters $T_H = 1200$ K, $T_L = 300$ K, $R = 1.1$ and $U_H/U_L = 1$ are chosen.

In order to further reveal the performance characteristics of an irreversible Braysson cycle, Eqs. (6), (7) and (10) are used to plot the $P^* \sim \eta$ curves, as shown in Fig. 4, where η_m and P^*_m are, respectively, the thermal efficiency at the maximum specific power output and the specific power output at the maximum thermal efficiency. The values of η_m are also listed in Table 1. It is seen from Fig. 4 that the specific power output is not a monotonic function of the thermal efficiency. When the specific power output is situated in the regions of the $P^* \sim \eta$ curves with a positive slope, it will decrease as the thermal efficiency is decreased. Obviously, these regions are not optimal. It is thus clear that the specific power output should be situated in the region of

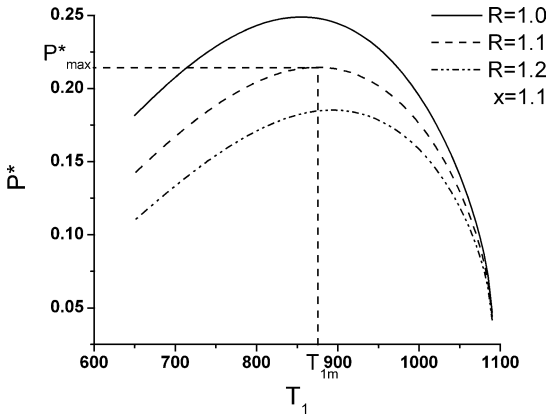

Fig. 3. The variation of the dimensionless specific power output P^* with respect to temperature T_1. The values of the parameters T_H, T_L and U_H/U_L are the same as those used in Fig. 2.

Table 1
The corresponding parameters at maximum specific power output

x	R	$P^*_{\max}$	η_m	T_{1m}	T_{3m}	$(A_H/A)_m$	$(A_L/A)_m$
1	1.0	0.250	0.472	900.000	450.000	0.500	0.500
	1.1	0.216	0.446	921.441	439.279	0.488	0.512
	1.2	0.186	0.422	940.994	429.503	0.477	0.523
1.1	1.0	0.249	0.470	854.897	449.660	0.498	0.502
	1.1	0.214	0.445	874.997	438.914	0.486	0.514
	1.2	0.185	0.420	893.279	429.111	0.475	0.525
1.2	1.0	0.246	0.467	810.557	448.771	0.495	0.505
	1.1	0.212	0.441	828.994	437.960	0.482	0.518
	1.2	0.182	0.416	845.657	428.090	0.470	0.530
1.3	1.0	0.242	0.462	768.091	447.496	0.489	0.511
	1.1	0.207	0.436	784.802	436.596	0.476	0.524
	1.2	0.178	0.410	799.785	426.635	0.463	0.537

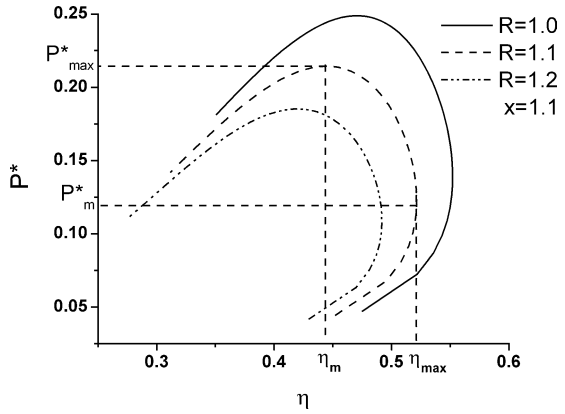

Fig. 4. The $P^* \sim \eta$ curves of a Braysson heat engine for $k_0/(U_L A) = 0.01$. The values of the parameters T_H, T_L and U_H/U_L are the same as those used in Fig. 2.

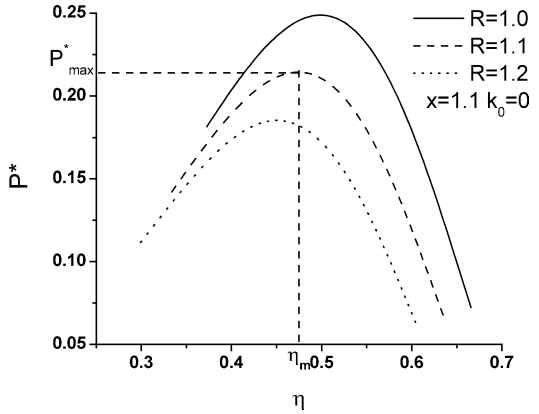

Fig. 5. The $P^* \sim \eta$ curves of a Braysson heat engine without the heat leak loss. The values of the parameters T_H, T_L and U_H/U_L are the same as those used in Fig. 2.

the $P^* \sim \eta$ curves with a negative slope. When the specific power output is in the region, it will increase as the thermal efficiency is decreased, and vice versa. Thus, the optimal regions of the specific power output and thermal efficiency should be subject to

$$P_m^* \leqslant P^* \leqslant P_{\max}^* \tag{11}$$

and

$$\eta_{\max} \geqslant \eta \geqslant \eta_m \tag{12}$$

This shows that $P_{\max}^*, \eta_{\max}, P_m^*$ and η_m are four important parameters of the Braysson heat engine. $P_{\max}^*$ and $\eta_{\max}$ give the upper bounds of the specific power output and corresponding thermal efficiency while P_m^* and η_m determine the allowable values of the lower bounds of the optimal specific power output and corresponding thermal efficiency.

According to Eqs. (11) and (12), we can further determine the optimal regions of other performance parameters. For example, the optimal regions of the parameters $T_1, T_3, A_H/A$ and A_L/A may be, respectively, determined by

$$T_{1m} \leqslant T_1 \leqslant T_{1\eta} \tag{13}$$

$$T_{3m} \geqslant T_3 \geqslant T_{3\eta} \tag{14}$$

$$(A_H/A)_m \leqslant (A_H/A) \leqslant (A_H/A)_\eta \tag{15}$$

and

$$(A_L/A)_m \geqslant (A_L/A) \geqslant (A_L/A)_\eta \tag{16}$$

where $T_{1m}, T_{3m}, (A_H/A)_m$ and $(A_L/A)_m$ are, respectively, the values of the $T_1, T_3, A_H/A$ and A_L/A at the maximum specific power output and have been listed in Table 1, and $T_{1\eta}, T_{3\eta}, (A_H/A)_\eta$ and $(A_L/A)_\eta$ are, respectively, the values of the $T_1, T_3, A_H/A$ and A_L/A at the maximum thermal efficiency and may be calculated numerically from the above equations.

So far we have obtained some optimum criteria for the important performance parameters of the cycle, which may provide some theoretical guidance for the design and improvement of the Braysson cycle.

5. Discussions

As mentioned above, some special cases of the cycle may be directly discussed from the results derived in this paper.

(1) When $R = 1$, the cycle becomes endoreversible. The characteristic curves of the Braysson heat engine are shown by the solid lines in Figs. 3 and 4.
(2) When $k_0 = 0$, the heat leak loss is not considered. In such a case, Figs. 2 and 3 are still true, because the specific power output is not affected by the heat leak loss between the heat reservoirs. However, the heat leak loss between the heat reservoirs will directly reduce the thermal efficiency of the cycle. When $k_0 = 0$, the $P^* \sim \eta$ curve of the cycle is not a closed loop line through the zero point but an approximate parabola line, as shown in Fig. 5.
(3) When $R = 1$ and $k_0 = 0$, we get the cycle model adopted in Refs. [2,3]. It implies the fact that some significant results in Refs. [2,3] may be directly obtained from this paper. For example, the $P^* \sim \eta$ curve plotted in Ref. [3] may be given by the solid line in Fig. 5 as long as the same values of the parameters are chosen.
(4) When $x = 1$, the cycle becomes the Carnot cycle [31–33] and Eqs. (6)–(9) may be, respectively, simplified as

$$P = \frac{U_H(1 - RT_3/T_2)}{1/(T_H - T_2) + (U_H/U_L)R[(T_3/T_2)/(T_3 - T_L)]} \tag{17}$$

$$\eta = \frac{1 - RT_3/T_2}{1 + \frac{k_0(T_H - T_L)}{U_H A}\left[\frac{1}{T_H - T_2} + \frac{U_H R T_3/T_2}{U_L(T_3 - T_L)}\right]} \tag{18}$$

$$\frac{A_H}{A} = \frac{1}{1 + \frac{U_H}{U_L}\frac{R(T_H - T_2)T_3/T_2}{T_3 - T_L}} \tag{19}$$

and

$$\frac{A_L}{A} = \frac{RT_3/(T_3 - T_L)}{\frac{U_L}{U_H}\frac{T_2}{T_H - T_2} + RT_3/(T_3 - T_L)} \tag{20}$$

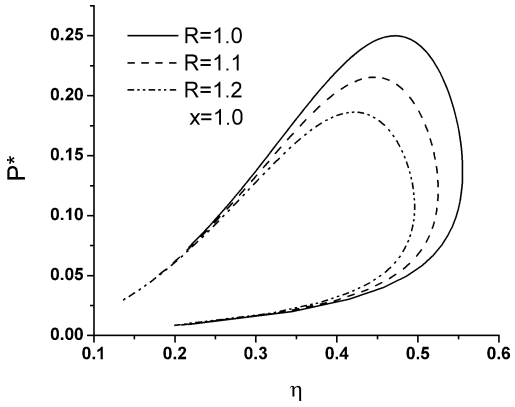

Fig. 6. The $P^* \sim \eta$ curves of a Carnot heat engine for $k_0/(U_L A) = 0.01$. The values of the parameters T_H, T_L and U_H/U_L are the same as those used in Fig. 2.

It shows clearly that the optimal performance of the Carnot heat engine can be directly obtained from the results derived in this paper. For example, using Eqs. (17) and (18), one can generate the $P^* \sim \eta$ characteristic curves of the cycle, as shown in Fig. 6.

(5) It is of interest to note that one may use not only the objective function [34] defined in Eq. (6) but also the objective function defined as [34]

$$P = \frac{Q_H - Q_L}{UA} = \frac{Q_H - Q_L}{U_H A_H + U_L A_L} = \frac{(x-1)T_1 - RT_3 \ln x}{a^* T_3/(T_3 - T_L) + b} \tag{21}$$

to optimize the performance of a heat engine, where $a^* = R \ln x$. Comparing Eq. (21) with Eq. (6), one can directly derive the performance characteristics of an irreversible Braysson heat engine optimized by the objective function defined in Eq. (21) through Eqs. (7)–(20), as long as U_H and U_L are chosen to be equal to 1 and A, A_H and A_L are replaced by $UA, U_H A_H$ and $U_L A_L$ in Eqs. (7)–(20), respectively.

6. Conclusions

An irreversible cycle model of a Braysson heat engine is established and used to investigate the influence of multi-irreversibilities on the performance of the heat engine. The specific power output is optimized with respect to the state point temperatures for a given set of other performance parameters. The maximum specific power output and some other important parameters are calculated for a typical set of operating conditions. The optimal regions of some important parameters such as the specific power output, thermal efficiency, temperatures of the working fluid, heat-transfer area ratios, and so on, are determined in detail. The influence of the isobaric temperature ratio x and internal irreversibility parameter R on the performance of the cycle is analyzed. Some special cases of the cycle are discussed so that the optimal performance of the Carnot heat engine may be directly derived from the results obtained in this paper. In other words, the analysis presented in this paper is general and will be useful to understand the relationships and difference between the Braysson cycle and other cycles and to further improve the optimal design and operation of a real Braysson heat engine for different sets of operating parameters and constraints.

Acknowledgement

One of the authors (SKT) is grateful to Xiamen University, Xiamen, People's Republic of China for providing the financial assistance and working opportunity during this study.

References

[1] T.H. Frost, A. Anderson, B. Agnew, A hybrid gas turbine cycle (Brayton/Ericsson): an alternative to conventional combined gas and steam turbine power plant, Proc. Inst. Mech. Engrs. Part A 211 (1997) 121–131.
[2] T. Zheng, L. Chen, F. Sun, C. Wu, Power, power density and efficiency optimization of an endoreversible Braysson cycle, Exergy Internat. J. 2 (2002) 380–386.
[3] J. Zheng, L. Chen, F. Sun, C. Wu, Powers and efficiency performance of an endoreversible Braysson cycle, Internat. J. Therm. Sci. 41 (2002) 201–205.
[4] C. Wu, Intelligent computer aided optimization of power and energy systems, Proc. Inst. Mech. Engrs. A 213 (1999) 1–6.
[5] S. Fujii, K. Kaneko, K. Otanl, Y. Tsujikawa, Mirror gas turbines: A newly proposed method of exhaust heat recovery, J. Engrg. Gas Turbines Power 123 (2001) 481–486.
[6] C. Wu, R.S. Kiang, Work and power optimization of a finite time Brayton cycle, Internat. J. Ambient Energy 11 (1990) 129–136.
[7] C. Wu, R.S. Kiang, Power performance of a nonisentropic Brayton cycle, J. Engrg. Gas Turbines Power 113 (1991) 501–504.
[8] H.S. Leff, Thermal efficiency at maximum power output: New results for old heat engines, Amer. J. Phys. 55 (1987) 602–610.
[9] O.M. Ibrahim, S.A. Klein, J.W. Mitchell, Optimum heat power cycles for specified boundary conditions, J. Engrg. Gas Turbines Power 113 (1991) 514–521.
[10] C. Wu, Specific power bounds of real heat engines, Energy Convers. Mgmt. 31 (1991) 249–253.
[11] C. Wu, Power optimization of an endoreversible Brayton gas turbine heat engine, Energy Convers. Mgmt. 31 (1991) 561–565.
[12] C. Wu, L. Chen, F. Sun, Performance of a regenerative Brayton heat engine, Energy 21 (1996) 71–76.
[13] C.Y. Cheng, C.K. Chen, Power optimization of an endoreversible regenerative Brayton cycle, Energy 21 (1996) 241–247.
[14] L. Chen, F. Sun, C. Wu, R.L. Kiang, Theoretical analysis of the performance of a regenerative closed Brayton cycle with internal irreversibilities, Energy Convers. Mgmt. 38 (1997) 871–877.
[15] V. Radcenco, J.V.C. Vargas, A. Bejan, Thermodynamic optimization of a gas turbine power plant with pressure drop irreversibilities, J. Energy Res. Tech. 120 (1998) 233–240.
[16] D.A. Blank, Analysis of a combined law power-optimized open Joule–Brayton heat-engine cycle with a finite interactive heat source, J. Phys. D: Appl. Phys. 32 (1999) 769–776.
[17] B. Sahin, A. Kodal, S.S. Kaya, A comparative performance analysis of irreversible regenerative reheating Joule–Brayton engines under

maximum power density and maximum power conditions, J. Phys. D: Appl. Phys. 31 (1998) 2125–2131.

[18] J.M.M. Roco, S. Velasco, A. Medina, A.C. Hernandez, Optimum performance of a regenerative Brayton thermal cycle, J. Appl. Phys. 82 (1997) 2735–2741.

[19] M. Feidt, Optimization of Brayton cycle engine in contract with fluid thermal capacities, Rev. Gen. Therm. 35 (1996) 662–666.

[20] L. Chen, N. Ni, G. Cheng, F. Sun, C. Wu, Performance of a real closed regenerated Brayton cycle via method of finite time thermodynamics, Internat. J. Ambient Energy 20 (1999) 95–104.

[21] C.Y. Cheng, C.K. Chen, Power optimization of an irreversible Brayton heat engine, Energy Sources 19 (1997) 461–474.

[22] D.A. Blank, C. Wu, A combined power optimized Joule–Brayton heat engine cycle with fixed thermal reservoir, Internat. J. Power Energy 20 (2000) 1–6.

[23] S.C. Kaushik, S.K. Tyagi, Finite time thermodynamic analysis of an irreversible regenerative closed cycle Brayton heat engine, Internat. J. Solar Energy 22 (2002) 141–151.

[24] D.A. Blank, C. Wu, Power limit of an endoreversible Ericsson cycle with regeneration, Energy Convers. Mgmt. 37 (1996) 59–66.

[25] D.A. Blank, C. Wu, Finite-time power limit for solar-radiant Ericsson engines in space applications, Appl. Thermal Engrg. 18 (1998) 1347–1357.

[26] J. Chen, J.A. Schouten, The comprehensive influence of several major irreversibilities on the performance of an Ericsson heat engine, Appl. Thermal Engrg. 19 (1999) 555–564.

[27] S.K. Tyagi, Application of finite time thermodynamics and second law evaluation of thermal energy conversion systems, Ph.D. Thesis, CCS. University, Meerut, India, 2000.

[28] S.C. Kaushik, S. Kumar, Finite time thermodynamic evaluation of irreversible Ericsson and Stirling heat engines, Energy Convers. Mgmt. 42 (2001) 295–312.

[29] F.L. Curzon, B. Ahlborn, Efficiency of a Carnot engine at maximum power output, Amer. J. Phys. 43 (1975) 22–24.

[30] A. Bejan, Theory of heat transfer-irreversible power plants, Internat. J. Heat Mass Transfer 31 (1988) 1211–1219.

[31] C. Wu, Maximum obtainable power of a Carnot combined power plant, Heat Recov. Syst. CHP 15 (1995) 351–355.

[32] J. Chen, The maximum power output and maximum efficiency of an irreversible Carnot heat engine, J. Phys. D: Appl. Phys. 27 (1994) 1144–1149.

[33] J. Chen, Thermodynamic and thermoeconomic analyses of an irreversible combined Carnot heat engine system, Internat. J. Energy Res. 25 (2001) 413–426.

[34] A. Bejan, Entropy generation minimization: The new thermodynamics of finite-size devices and finite time processes, J. Appl. Phys. 79 (1996) 1191–1218.

[35] K.H. Hoffmann, J.M. Burzler, S. Schubert, Endoreversible thermodynamics, J. Non-Equilib. Thermodyn. 22 (1997) 311–355.

[36] L. Chen, C. Wu, F. Sun, Finite time thermodynamic optimization or entropy generation minimization of energy systems, J. Non-Equilib. Thermodyn. 24 (1999) 327–359.

[37] R.S. Berry, V.A. Kazakov, S. Sieniutycz, Z. Szwast, A.M. Tsirlin, Thermodynamic Optimization of Finite Time Processes, Wiley, Chichester, 1999.

[38] C. Wu, L. Chen, J. Chen (Eds.), Recent Advances in Finite Time Thermodynamics, Nova Science, New York, 1999.